Journal of Computational Physics **167,** 72–98 (2001)
doi:10.1006/jcph.2000.6659, available online at http://www.idealibrary.com on IDEAL®

An Extended FDTD Scheme for the Wave Equation: Application to Multiscale Electromagnetic Simulation[1]

Jean-Luc Vay

Lawrence Berkeley National Laboratory, Accelerator and Fusion Research Division, 1 Cyclotron Road, Berkeley, California 94720
E-mail: jlvay@lbl.gov

Received March 10, 2000; revised September 12, 2000

An algorithm for the application of the mesh refinement technique to finite-difference calculation of the wave equation is presented via the introduction of a new "extended" FDTD scheme. This scheme can be viewed as an extension of the Yee scheme using a new set of variables relating to the direction of propagation of the waves along an axis. Because of this additional information, this scheme allows a more natural implementation of the mesh refinement technique. The extended scheme is presented for both a one-dimensional and a multidimensional system. The mesh refinement algorithm is given in one dimension, and the performances are compared to other proposed schemes.

Key Words: finite-difference; mesh refinement; electromagnetic; wave equation; FDTD; domain decomposition.

1. INTRODUCTION

The finite-difference time-domain technique is widely used to solve the wave equation numerically, especially in the form of the Yee algorithm [2] which relies on centered finite difference of field quantities defined on a staggered mesh. This algorithm is limited, however, to a uniform Cartesian mesh. In this article, we present a method of incorporating the mesh refinement technique. Mesh refinement involves a sudden jump of resolution at the interface of two grids with different mesh sizes. Hence, a wave traveling across this interface will have two different experiences depending on its direction of propagation perpendicular to the interface. It will enter a region of either finer or coarser resolution. In the first case, all wavelengths should be transmitted, whereas in the second case, all wavelengths that are not resolved on the coarser grid should be absorbed at the interface. It is not obvious a

[1] Supported by the Office of Fusion Energy, U.S. Department of Energy, under Contract DEACO3-765F00098.

0021-9991/01 $35.00

priori that an algorithm identically treating both directions of propagation (e.g., as the Yee algorithm) can handle these requirements. Our strategy is to define a more general algorithm (containing the Yee scheme as a particular case) which treats the signal differently depending on its direction of propagation along one of the principal axis of calculation, allowing the mesh refinement technique to be incorporated naturally. If needed, a method of coupling this "extended" (or "directional") algorithm to the Yee scheme has been developed and will be presented in another article.

This article is divided in two parts. In the first part, we define and analyze the properties of the extended scheme. In the second part, we develop a boundary condition for the use of mesh refinement with the extended scheme.

In the first part, we begin by deriving the extended scheme for a 1D system. From general considerations, we define the mathematical form of the solution and show that, at the lowest level of approximation, the solution corresponds to an algorithm with three independent parameters. It is shown that this algorithm is very general and reduces to well-known algorithms (such as the Yee scheme, the one-way absorbing boundary condition [5], or the Berenger PML [1]) for some values of these parameters. A relation linking the parameters is then derived from the properties of the wave equation, and it is shown that, unless specific conditions apply, two different relations hold depending on the direction of propagation of the wave. This result is used in the next section to justify (at least theoretically) the development of the extended scheme, which is then defined and derived in its infinitesimal and finite-difference forms. The scheme is extended to a system of higher dimensionality by a decomposition of the overall system into one-dimensional wave equations, allowing the direct applications of the algorithm developed in the preceding section. For application to electromagnetic calculations, a link between the extended scheme and Maxwell equations is established.

In the second part of the article, a boundary condition for the use of the mesh refinement technique with the extended scheme is developed in one dimension, first in the case of spatial refinement only and then in the case of space–time refinement. The performances of both schemes are compared to those of possible schemes which are not "directional." It is recalled that "undirectional" algorithms are potentially unstable for "sandwich" configurations (a fine grid embedded between two coarse grids), a very likely configuration for practical use, because of high-frequency trapping (and possible amplification). Our directional scheme avoids by construction this instability.

1.1. Notations

We will consider a quantity A discretized on a space–time regular grid and noted A^i_j, A^i_{jk}, or A^i_{jkl} for, respectively, a 1-, 2-, or 3-dimensional system and where i is the time index and j, k, l are the space indices along x, y, and z, respectively.

One defines the discrete operators of finite-difference Δ^t and Δ^x and the operators of finite-average $\langle E\rangle_t$ and $\langle E\rangle_x$ as

$$\Delta^t \equiv \frac{A^{i+1}_j - A^i_j}{\delta t}; \qquad \Delta^x \equiv \frac{A^i_{j+1} - A^i_j}{\delta x} \tag{1}$$

$$\langle E\rangle_t \equiv \frac{A^{i+1}_j + A^i_j}{2}; \quad \langle E\rangle_x \equiv \frac{A^i_{j+1} + A^i_j}{2}, \tag{2}$$

where δt and δx are the time step and mesh size along x, y, and z, respectively.

2. PART I: DESCRIPTION OF THE EXTENDED SCHEME

2.1. In One Dimension

We consider the centered finite-difference discretization of the wave equation

$$\frac{\partial^2 E}{\partial t^2} = \frac{\partial^2 E}{\partial x^2} \equiv \left\{ \frac{\partial E}{\partial t} = \frac{\partial B}{\partial x}; \frac{\partial B}{\partial t} = \frac{\partial E}{\partial x} \right\} \tag{3}$$

on a staggered mesh (see Fig. 1). We assume that the solution of E^{i+1} is explicit (i.e., it does not depend on terms with $i+1$ or more) and is a linear function of the form

$$\begin{aligned} E_j^{i+1} = {} & \alpha_1 E_j^i + \beta_{11} B_{j+1/2}^{i+1/2} - \beta_{12} B_{j-1/2}^{i+1/2} + \beta_{13} B_{j+3/2}^{i+1/2} - \beta_{14} B_{j-3/2}^{i+1/2} \cdots \\ & + \alpha_2 E_j^{i-1} + \beta_{21} B_{j+1/2}^{i-1/2} - \beta_{22} B_{j-1/2}^{i-1/2} + \beta_{23} B_{j+3/2}^{i-1/2} - \beta_{24} B_{j-3/2}^{i-1/2} \cdots \\ & \cdots \\ & \cdots \\ & \cdots \end{aligned} \tag{4}$$

For numerical reasons, the algorithm should be as local (in time and in space) as possible, and we consider in this paper the subset

$$E_j^{i+1} = \alpha E_j^i + \beta_1 B_{j+1/2}^{i+1/2} - \beta_2 B_{j-1/2}^{i+1/2}. \tag{5}$$

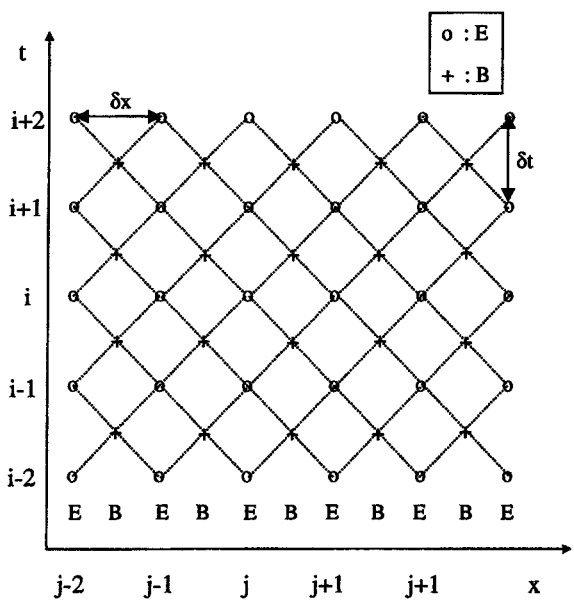

FIG. 1. Diagram showing the positions of E and B on the discrete space–time grid. E and B are staggered both in space and in time.

Remark. This finite-difference equation is the centered finite-difference discretization of the infinitesimal equation

$$\frac{\partial E}{\partial t} = \sigma_E E + \frac{\partial B}{\partial x} + \sigma_B B, \tag{6}$$

since it rewrites as

$$\frac{E_j^{i+1} - E_j^i}{\delta t} = \sigma_E \frac{E_j^{i+1} + E_j^i}{2} + \frac{B_{j+1/2}^{i+1/2} - B_{j-1/2}^{i+1/2}}{\delta x} + \sigma_B \frac{B_{j+1/2}^{i+1/2} + B_{j-1/2}^{i+1/2}}{2} \tag{7}$$

or

$$\Delta^t E = \sigma_E \langle E \rangle_t + \Delta^x B + \sigma_B \langle B \rangle_x, \tag{8}$$

with

$$\begin{cases} \sigma_E = \frac{2}{\delta t}\left(\frac{\alpha - 1}{\alpha + 1}\right) \\ \frac{1}{\delta x} = \frac{1}{\delta t}\left(\frac{\beta_1 + \beta_2}{\alpha + 1}\right) \\ \sigma_B = \frac{2}{\delta t}\left(\frac{\beta_1 - \beta_2}{\alpha + 1}\right). \end{cases} \tag{9}$$

Remark. This formulation reduces to well-known algorithms for particular values of the set of parameters $(\alpha, \beta_1, \beta_2)$ or $(\sigma_E, \delta x, \sigma_B)$. For example, it reduces to

- the Yee scheme

$$E_j^{i+1} = E_j^i + \frac{\delta t}{\delta x}\left(B_{j+1/2}^{i+1/2} - B_{j-1/2}^{i+1/2}\right) \tag{10}$$

for $(\alpha, \beta_1, \beta_2) = (1, \frac{\delta t}{\delta x}, \frac{\delta t}{\delta x})$,

- the one-way "Sommerfeld" outgoing-wave boundary condition

$$E_j^{i+1} = \left(1 - \frac{2\delta t}{\delta t + \delta x}\right) E_j^i - \frac{2\delta t}{\delta t + \delta x} B_{j-1/2}^{i+1/2} \tag{11}$$

with $(\alpha, \beta_1, \beta_2) = (1 - \frac{2\delta t}{\delta t + \delta x}, 0, \frac{2\delta t}{\delta t + \delta x})$ for waves traveling forward and

$$E_j^{i+1} = \left(1 - \frac{2\delta t}{\delta t + \delta x}\right) E_j^i + \frac{2\delta t}{\delta t + \delta x} B_{j+1/2}^{i+1/2} \tag{12}$$

with $(\alpha, \beta_1, \beta_2) = (1 - \frac{2\delta t}{\delta t + \delta x}, \frac{2\delta t}{\delta t + \delta x}, 0)$ for waves traveling backward,

- the Berenger multilayer PML boundary condition

$$\frac{E_j^{i+1} - E_j^i}{\delta t} = \sigma \frac{E_j^{i+1} + E_j^i}{2} + \frac{B_{j+1/2}^{i+1/2} - B_{j-1/2}^{i+1/2}}{\delta x} \tag{13}$$

for $(\sigma_E, \delta x, \sigma_B) = (\sigma, \delta x, 0)$.

Remark. We can reinterpret the one-way boundary condition using this formalism as follows.

When considering the sets $(\sigma_E, \delta x, \sigma_B)$ corresponding to the sets $(\alpha, \beta_1, \beta_2)$ of the one-way absorbing condition, we have

$$\begin{aligned}(\alpha,\beta_1,\beta_2) &= \left(1-\frac{2\delta t}{\delta t+\delta x}, 0, \frac{2\delta t}{\delta t+\delta x}\right) \Leftrightarrow (\sigma_E,\delta x,\sigma_B) = \left(-\frac{2}{\delta x}, \delta x, -\frac{2}{\delta x}\right)\\ (\alpha,\beta_1,\beta_2) &= \left(1-\frac{2\delta t}{\delta t+\delta x}, \frac{2\delta t}{\delta t+\delta x}, 0\right) \Leftrightarrow (\sigma_E,\delta x,\sigma_B) = \left(-\frac{2}{\delta x}, \delta x, \frac{2}{\delta x}\right).\end{aligned} \tag{14}$$

Plugging these coefficients into (7), we retrieve the one-way absorbing condition. Because this is an approximation of the wave equation, we can consider that $E = -B$ for waves propagating forward and $E = B$ for waves propagating backward. This gives (with $\sigma = \sigma_E = \pm\sigma_B = -\frac{2}{\delta x}$)

$$\frac{E_j^{i+1}-E_j^i}{\delta t} = \sigma\frac{E_j^{i+1}+E_j^i}{2} + \frac{B_{j+1/2}^{i+1/2}-B_{j-1/2}^{i+1/2}}{\delta x} - \sigma\frac{E_{j+1/2}^{i+1/2}+E_{j-1/2}^{i+1/2}}{2}, \tag{15}$$

which is the discretization of

$$\frac{\partial E}{\partial t} = \sigma E + \frac{\partial B}{\partial x} - \sigma E. \tag{16}$$

We see then that we can interpret the 1D one-way absorbing condition as the centered finite-difference discretization of a redundant form of the wave equation. Two terms (σE and $-\sigma E$), which cancel each other at the infinitesimal limit, are added to the equation. The first term is computed as an average in time $\sigma E \equiv 0.5\sigma(E_j^{i+1}+E_j^i)$, while the latter is computed as an average in space $-\sigma E \equiv -0.5\sigma(E_{j+1/2}^{i+1/2}+E_{j-1/2}^{i+1/2})$. The use of the relations $E = -B$ and $E = B$ for the waves propagating forward and backward, respectively, gives the final one-way absorbing algorithm. Identically, we can derive an ingoing-wave boundary condition by reversing the sign of σ.

2.1.1. *A Simple Relation Linking the Coefficients*

As we will show now, a simple relation, coming from the properties of the wave equation, links the coefficients α, β_1, and β_2.

If we consider the propagation of an Heaviside step of amplitude H traveling forward, we do not know the details of the response of the system for any set $(\alpha, \beta_1, \beta_2)$ but we know from the properties of the wave equation that, after an infinite time, all the values must have exactly relaxed to the value H for the magnetic field B and $-H$ for the electric field E (we have $E = -B$ for waves traveling forward), giving the relation (true after an infinite time), from Eq. (5),

$$-H = -\alpha H + \beta_1 H - \beta_2 H, \tag{17}$$

and finally,

$$\alpha = 1 + \beta_1 - \beta_2. \tag{18}$$

The same analysis with waves traveling backward gives

$$\alpha = 1 - \beta_1 + \beta_2. \tag{19}$$

These relations hold in vacuum, and we can check that they are verified in the following cases.

- The Yee scheme: $(\alpha, \beta_1, \beta_2) = (1, \frac{\delta t}{\delta x}, \frac{\delta t}{\delta x})$.
- The one-way absorbing conditions: $(\alpha, \beta_1, \beta_2) = (1 - \frac{2\delta t}{\delta t + \delta x}, 0, \frac{2\delta t}{\delta t + \delta x})$ for waves propagating forward or $(\alpha, \beta_1, \beta_2) = (1 - \frac{2\delta t}{\delta t + \delta x}, \frac{2\delta t}{\delta t + \delta x}, 0)$ for waves propagating backward.

In the formalism of Eq. (8), the conditions become, plugging (18) and (19), respectively, into (9)

$$\sigma_B = \sigma_E \quad \text{for waves traveling forward} \tag{20}$$

$$\sigma_B = -\sigma_E \quad \text{for waves traveling backward.} \tag{21}$$

2.1.2. *A "Directional" System of Equations*

The preceding analysis shows that, unless $\beta_1 = \beta_2$ (which is true only when $\sigma_B = \sigma_E = 0$ in (7)), two different equations apply to the descriptions of waves going forward and backward. For this reason, we will develop now what we call a "directional" (or "extended") system of equations in order to describe fully the system for any values of β_1 and β_2.

We will describe the wave equation in vacuum

$$\begin{aligned} \frac{\partial B}{\partial t} = \frac{\partial E}{\partial x} &\equiv \frac{\partial B}{\partial t} = \sigma_B B + \frac{\partial E}{\partial x} - \sigma_B B \\ \frac{\partial E}{\partial t} = \frac{\partial B}{\partial x} - J &\equiv \frac{\partial E}{\partial t} = \sigma_E E + \frac{\partial B}{\partial x} - \sigma_E E - J. \end{aligned} \tag{22}$$

The second set is clearly equivalent to the first one; we have simply added and substracted the same term. Although this will have an effect at the discretized level, it has no effect at the infinitesimal level, ensuring that we will really approximate the wave equation.

Let us call E^+ and B^+ the electric and magnetic fields of waves going forward and E^- and B^- the electric and magnetic fields of waves going backward, and use the equivalent set

$$\begin{aligned} E &= E^+ + E^- \\ \delta E &= E^+ - E^- \\ B &= B^+ + B^- \\ \delta B &= B^+ - B^-. \end{aligned} \tag{23}$$

Because we have the relations $E^+ = -B^+$ and $E^- = B^-$, we also have $E = -\delta B$ and $B = -\delta E$, and we can rewrite (22) as

$$\begin{aligned} \frac{\partial B}{\partial t} &= \sigma_B B + \frac{\partial E}{\partial x} + \sigma_B \delta E \\ \frac{\partial E}{\partial t} &= \sigma_E E + \frac{\partial B}{\partial x} + \sigma_E \delta B - J. \end{aligned} \tag{24}$$

Still using the relations $E = -\delta B$ and $B = -\delta E$, this gives, for δE and δB,

$$\begin{aligned} \frac{\partial \delta E}{\partial t} &= \sigma_E \delta E + \frac{\partial \delta B}{\partial x} + \sigma_E B \\ \frac{\partial \delta B}{\partial t} &= \sigma_B \delta B + \frac{\partial \delta E}{\partial x} + \sigma_B E + J. \end{aligned} \tag{25}$$

The systems (24) and (25) form a complete set of equations for the set of variables $(E, \delta E, B, \delta B)$, which can be discretized as

$$\begin{aligned} \Delta_t B &= \sigma_B \langle B \rangle_t + \Delta_x E + \sigma_B \langle \delta E \rangle_x \\ \Delta_t E &= \sigma_E \langle E \rangle_t + \Delta_x B + \sigma_E \langle \delta B \rangle_x - J \\ \Delta_t \delta E &= \sigma_E \langle \delta E \rangle_t + \Delta_x \delta B + \sigma_E \langle B \rangle_x \\ \Delta_t \delta B &= \sigma_B \langle \delta B \rangle_t + \Delta_x \delta E + \sigma_B \langle E \rangle_x + \langle \langle J \rangle_x \rangle_t. \end{aligned} \tag{26}$$

A detailed analysis of this system (see Appendix), when in steady-state with a constant source J, shows that a term must be added in the discretized system for consistency: The set then becomes

$$\begin{aligned} \Delta_t B &= \sigma_B \langle B \rangle_t + \Delta_x E + \sigma_B \langle \delta E \rangle_x + \sigma_B \Delta_x \langle J \rangle_t \\ \Delta_t E &= \sigma_E \langle E \rangle_t + \Delta_x B + \sigma_E \langle \delta B \rangle_x - J \\ \Delta_t \delta E &= \sigma_E \langle \delta E \rangle_t + \Delta_x \delta B + \sigma_E \langle B \rangle_x \\ \Delta_t \delta B &= \sigma_B \langle \delta B \rangle_t + \Delta_x \delta E + \sigma_B \langle E \rangle_x + \langle \langle J \rangle_x \rangle_t. \end{aligned} \tag{27}$$

The new term $\Delta_x \langle J \rangle_t$ is purely numeric; it tends toward zero at the infinitesimal limit.

Because of the terms $\Delta_x \langle J \rangle_t$ and $\langle \langle J \rangle_x \rangle_t$, this system is not fully explicit and may present some difficulty for the implementation. For this reason, we derive an equivalent system that is fully explicit.

We first determine the finite-difference form of $\partial \delta B / \partial t$ from $\partial B / \partial t$ using $B = B^+ + B^-$. From

$$\frac{\partial B}{\partial t} = \sigma_B B + \frac{\partial E}{\partial x} + \sigma_B \delta E \tag{28}$$

we get

$$\frac{\partial B^+}{\partial t} = \sigma_B B^+ + \frac{\partial E^+}{\partial x} + \sigma_B E^+ \tag{29}$$

$$\frac{\partial B^-}{\partial t} = \sigma_B B^- + \frac{\partial E^-}{\partial x} - \sigma_B E^- \tag{30}$$

and the discretization gives

$$\Delta_t B^+ = \sigma_B \langle B^+ \rangle_t + \Delta_x E^+ + \sigma_B \langle E^+ \rangle_x \tag{31}$$

$$\Delta_t B^- = \sigma_B \langle B^- \rangle_t + \Delta_x E^- - \sigma_B \langle E^- \rangle_x. \tag{32}$$

Let us decompose the field E in a propagative part E_w and a nonpropagative source part E_s such that, for a source J located at j_0, we have $E_w = E_w^+ + E_w^- = E^+(j > j_0) + E^-(j < j_0)$ and $E_s = E_s^+ + E_s^- = E^+(j = j_0) + E^-(j = j_0)$. (Remark: because of isotropy of the system, we have $E^+(j = j_0) = E^-(j = j_0)$.)

The variable $\delta E = E^+ - E^-$ is rewritten as $\delta E = \delta E_w + \delta E_s$, where

$$\delta E_w = E^+(j > j_0) - E^-(j < j_0) \tag{33}$$

and

$$\delta E_s = E^+(j = j_0) - E^-(j = j_0) = 0. \tag{34}$$

We remark that

$$E = E_w + E_s \tag{35}$$

$$\delta E = \delta E_w + \delta E_s = \delta E_w. \tag{36}$$

From (29) and (30), we can write

$$\Delta_t B^+ = \sigma_B \langle B^+ \rangle_t + \Delta_x (E_w^+ + E_s^+) + \sigma_B \langle E_w^+ + E_s^+ \rangle_x \tag{37}$$

$$\Delta_t B^- = \sigma_B \langle B^- \rangle_t + \Delta_x (E_w^- + E_s^-) - \sigma_B \langle E_w^- + E_s^- \rangle_x. \tag{38}$$

For a δB located at $j + 1/2$, the source of a signal propagating forward will be located at j (so that $E_s^+(j+1) = 0$), while the source of a signal propagating backward will be located at $j + 1$ (so that $E_s^-(j) = 0$). We can write more explicitly

$$\begin{aligned} \Delta_t B^+ = {} & \sigma_B \langle B^+ \rangle_t + \left(E_{w\,j+1}^{+\,i+1} - E_{w\,j}^{+\,i+1} - E_{s\,j}^{+\,i+1}\right)/\delta x \\ & + \sigma_B \left(E_{w\,j+1}^{+\,i+1} + E_{s\,j+1}^{+\,i+1} + E_{w\,j}^{+\,i+1} + E_{s\,j}^{+\,i+1}\right)/2 \end{aligned} \tag{39}$$

$$\begin{aligned} \Delta_t B^- = {} & \sigma_B \langle B^- \rangle_t + \left(E_{w\,j+1}^{-\,i+1} + E_{s\,j+1}^{-\,i+1} - E_{w\,j}^{-\,i+1}\right)/\delta x \\ & - \sigma_B \left(E_{w\,j+1}^{-\,i+1} + E_{s\,j+1}^{-\,i+1} + E_{w\,j}^{-\,i+1} + E_{s\,j}^{-\,i+1}\right)/2 \end{aligned} \tag{40}$$

or

$$\begin{aligned} \Delta_t B^+ = {} & \sigma_B \langle B^+ \rangle_t + \left(E_{w\,j+1}^{+\,i+1} - E_{w\,j}^{+\,i+1}\right)/\delta x \\ & + \sigma_B \left(E_{w\,j+1}^{+\,i+1} + E_{s\,j+1}^{+\,i+1} + E_{w\,j}^{+\,i+1} + E_{s\,j}^{+\,i+1}\right)/2 - E_{s\,j}^{+\,i+1}/\delta x \end{aligned} \tag{41}$$

$$\begin{aligned} \Delta_t B^- = {} & \sigma_B \langle B^- \rangle_t + \left(E_{w\,j+1}^{-\,i+1} - E_{w\,j}^{-\,i+1}\right)/\delta x \\ & - \sigma_B \left(E_{w\,j+1}^{-\,i+1} + E_{s\,j+1}^{-\,i+1} + E_{w\,j}^{-\,i+1} + E_{s\,j}^{-\,i+1}\right)/2 + E_{s\,j+1}^{-\,i+1}/\delta x. \end{aligned} \tag{42}$$

Subtracting the two, we get

$$\begin{aligned} \Delta_t \delta B = {} & \sigma_B \langle \delta B \rangle_t + \left(\delta E_{w\,j+1}^{i+1} - \delta E_{w\,j}^{i+1}\right)/\delta x \\ & + \sigma_B \left(E_{w\,j+1}^{i+1} + E_{s\,j+1}^{i+1} + E_{w\,j}^{i+1} + E_{s\,j}^{i+1}\right)/2 - \left(E_{s\,j}^{+\,i+1} + E_{s\,j+1}^{-\,i+1}\right)/\delta x. \end{aligned} \tag{43}$$

Using (35) and (36), this can be rewritten in the more compact form

$$\Delta_t \delta B = \sigma_B \langle \delta B \rangle_t + \Delta_x \delta E + \sigma_B \langle E \rangle_x - \frac{2\langle E_s \rangle_x}{\delta x}. \tag{44}$$

Applying the same analysis to the numerical correction in $B(t)$, we finally obtain the system

$$\begin{aligned}
\Delta_t B &= \sigma_B \langle B\rangle_t + \Delta_x E + \sigma_B \langle \delta E\rangle_x - 0.5\sigma_B \Delta_x E_s \\
\Delta_t E &= \sigma_E \langle E\rangle_t + \Delta_x B + \sigma_E \langle \delta B\rangle_x - J \\
\Delta_t \delta E &= \sigma_E \langle \delta E\rangle_t + \Delta_x \delta B + \sigma_E \langle B\rangle_x \\
\Delta_t \delta B &= \sigma_B \langle \delta B\rangle_t + \Delta_x \delta E + \sigma_B \langle E\rangle_x - \frac{2\langle E_s\rangle_x}{\delta_x}.
\end{aligned} \tag{45}$$

We still have no equation to update E_s in this system. Because of (36), δE contains no information on E_s, and this one cannot be retrieved from a linear combination of E and δE. Ideally, a wave equation should be solved for each E_s. This is practically impossible. Instead, we truncate the wave equation to solve for each E_s with a one-way ABC. We compute E_s as

$$\begin{aligned}
\Delta_t E_s &= 2 \cdot B_s/\delta x - J \\
\Delta_t B_s &= -\frac{2}{\delta x}\langle B_s\rangle_t - 2E_s/\delta x.
\end{aligned} \tag{46}$$

We created only one extra variable B_s on which we apply the one-way ABC.

The two systems (45) and (46) form a complete set, which is fully explicit.

2.1.3. *Properties of the System*

Dispersion relation. All the equations in (45) have the same form, and so we can restrict ourselves to the analysis of only one of them (the terms $0.5\sigma_B \Delta_x E_s$, J and $\frac{2\langle E_s\rangle_x}{\delta x}$ are source terms that do not affect the present analysis).

Considering the equation

$$\Delta_t E = \sigma \langle E\rangle_t + \Delta_x B + \sigma \langle \delta B\rangle_x \tag{47}$$

and assuming the propagation of a wave of the form $E_0 e^{i(\omega t - kx)}$, we obtain the dispersion relation (considering that $E = -\delta B$)

$$\frac{\sin\left(\frac{\omega\delta t}{2}\right)}{\delta t} - \frac{\sin\left(\frac{k\delta x}{2}\right)}{\delta x} + 0.5\sigma i \cos\left(\frac{\omega\delta t}{2}\right) - 0.5\sigma i \cos\left(\frac{k\delta x}{2}\right) = 0, \tag{48}$$

or equivalently,

$$r^2 - Br - C = 0, \tag{49}$$

which gives an analytic solution for $\omega(k)$ of the form

$$\omega = -\frac{2i}{\delta t}\ln r, \tag{50}$$

where

$$r = 0.5(B \pm \sqrt{B^2 + 4C}), \tag{51}$$

with

$$B = \frac{\delta t/\delta x}{1 - \sigma\delta t/2}\left(e^{ik\delta x/2} - e^{-ik\delta x/2}\right) - \frac{\sigma\delta t/2}{1 - \sigma\delta t/2}\left(e^{ik\delta x/2} + e^{-ik\delta x/2}\right) \tag{52}$$

$$C = \frac{1 + \sigma\delta t/2}{1 - \sigma\delta t/2}. \tag{53}$$

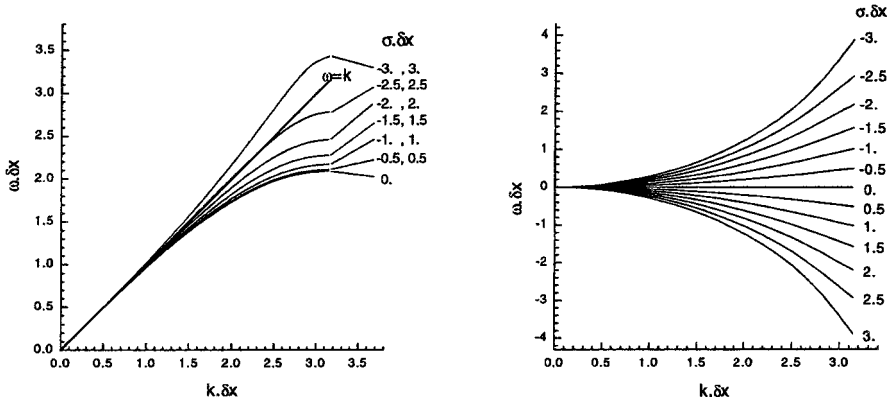

FIG. 2. Dispersion relation solution (real and imaginary parts) of the extended scheme, σ varying between $-3/\delta x$ and $3/\delta x$. There is damping for $\sigma < 0$ and instability for $\sigma > 0$.

The analytic solution for (51) using the positive sign[2] was used to plot the curves $\omega(k)$ on Fig. 2 for σ varying between $-3./\delta x$ and $3./\delta x$.

Considering the real part, when the modulus of σ increases, the speed of waves becomes closer to the continuous limit ($\omega = k$), up to a certain value of σ, where the curves become entirely above the $\omega = k$ curve. Considering the imaginary part, there is some damping (increasing with frequency) for σ negative while the system becomes unstable for σ positive. The reason for the instability can be intuitively understood by remarking that when this form of the general equation,

$$E_j^{i+1} = \alpha E_j^i + \beta\left(B_{j+1/2}^{i+1/2} - B_{j-1/2}^{i+1/2}\right) + \gamma\left(\delta B_{j+1/2}^{i+1/2} + \delta B_{j-1/2}^{i+1/2}\right), \tag{54}$$

where

$$\alpha = \frac{1+\sigma\Delta t/2}{1-\sigma\Delta t/2}, \tag{55}$$

is considered, σ positive corresponds to α greater than 1.

Setting σ to a negative value will help to provide simulations that are less noisy by damping high frequencies (see example in 2D below). This will also help, along with the fact that the speed of high-frequency waves (real part) is closer to its correct value, to reduce the numerical Cerenkov instability that may occur with relativistic particles [7].

Absorbing boundary condition. When the equation

$$\frac{E_j^{i+1} - E_j^i}{\delta t} = \sigma\frac{E_j^{i+1} + E_j^i}{2} + \frac{B_{j+1/2}^{i+1/2} - B_{j-1/2}^{i+1/2}}{\delta x} - \sigma\frac{\delta B_{j+1/2}^{i+1/2} + \delta B_{j-1/2}^{i+1/2}}{2} \tag{56}$$

is considered, the term $B_{j+1/2}^{i+1/2}$ or $B_{j-1/2}^{i+1/2}$ disappears for $\sigma = -2/\delta x$ (depending on the direction of the wave propagation), giving the relations

$$E_j^{i+1} = \left(1 - \frac{2\delta t}{\delta t + \delta x}\right)E_j^i + \left(\frac{2\delta t}{\delta t + \delta x}\right)B_{j+1/2}^{i+1/2} \tag{57}$$

[2] The solution with the minus sign is known as the "parasitic" solution (see [6]); as it does not change our general conclusions, we neglect further consideration.

for waves propagating backward and

$$E_j^{i+1} = \left(1 - \frac{2\delta t}{\delta t + \delta x}\right) E_j^i - \left(\frac{2\delta t}{\delta t + \delta x}\right) B_{j-1/2}^{i+1/2} \tag{58}$$

for waves propagating forward. Equation (57) can be used at the left boundary and Eq. (58) at the right boundary to absorb outgoing waves.

2.2. Extension to Higher Dimension

We now develop a scheme that we apply to a wave equation and not directly to Maxwell equations. To avoid confusion, we change notation and consider a wave equation on the scalar variable $f(x, y, z)$ with an intermediate vector variable $\vec{g}(x, y, z) = [g_x, g_y, g_z](x, y, z)$. The extension to Maxwell equations is explained in a following section.

The scheme that we have developed in the preceding section applies to a one-dimensional system. The extension to a higher dimension implies that, for one direction, all the information coming from the coupling with another direction is included in the source term. A three-dimensional wave equation of the form

$$\frac{\partial^2 f}{\partial t^2} = \frac{\partial^2 f}{\partial x^2} + \frac{\partial^2 f}{\partial y^2} + \frac{\partial^2 f}{\partial z^2} + \frac{\partial S}{\partial t} \tag{59}$$

can be rewritten as a set of first-order derivative equations as

$$\begin{aligned} \frac{\partial f}{\partial t} &= \vec{\nabla} \cdot \vec{g} + S \\ \frac{\partial \vec{g}}{\partial t} &= \vec{\nabla} f, \end{aligned} \tag{60}$$

where $\vec{g} = (g_x, g_y, g_z)$. Defining

$$\begin{aligned} s_x &= \frac{\partial g_y}{\partial y} + \frac{\partial g_z}{\partial z} + S \\ s_y &= \frac{\partial g_x}{\partial x} + \frac{\partial g_z}{\partial z} + S \\ s_z &= \frac{\partial g_x}{\partial x} + \frac{\partial g_y}{\partial y} + S, \end{aligned} \tag{61}$$

we can rewrite (60) as

$$\begin{aligned} \frac{\partial f}{\partial t} &= \frac{\partial g_x}{\partial x} + s_x = \frac{\partial g_y}{\partial y} + s_y = \frac{\partial g_z}{\partial z} + s_z \\ \frac{\partial g_x}{\partial t} &= \frac{\partial f_{/x}}{\partial x} \\ \frac{\partial g_y}{\partial t} &= \frac{\partial f_{/y}}{\partial y} \\ \frac{\partial g_z}{\partial t} &= \frac{\partial f_{/z}}{\partial z}, \end{aligned} \tag{62}$$

where $f_{/x} = \frac{\partial g_x}{\partial x} + s_x = f$, $f_{/y} = \frac{\partial g_y}{\partial y} + s_y$ and $f_{/z} = \frac{\partial g_z}{\partial z} + s_z$.

This forms a system of three sets of monodimensional wave equations along x, y, and z. For each system, the coupling with the other directions is formally enclosed in the source term. A more compact vectorial notation is given by

$$\begin{aligned}\frac{\partial f}{\partial t} &= \vec{\nabla}\cdot\vec{g} + S\\ \frac{\partial \vec{g}}{\partial t} &= \vec{\nabla} f\\ \vec{s} &= [\vec{\nabla}\cdot\vec{g} + S]\hat{u} - \vec{\vec{\nabla}}\cdot\vec{g} = \frac{\partial f}{\partial t}\hat{u} - \vec{\vec{\nabla}}\cdot\vec{g},\end{aligned} \tag{63}$$

with $\vec{s} = (s_x, s_y, s_z)$, $\vec{u} = (x, y, z)$, $\hat{u} = \vec{u}/|u|$, and

$$\vec{\vec{\nabla}} = \begin{pmatrix} \frac{\partial}{\partial x} & 0 & 0\\ 0 & \frac{\partial}{\partial y} & 0\\ 0 & 0 & \frac{\partial}{\partial z}\end{pmatrix}.$$

2.2.1. *Extended Scheme Formulation*

In the continuous limit. Having now monodimensional equations, we can apply the extended algorithm described previously in (24) and (25). We define $\delta f_x, \delta f_y, \delta f_z, \delta g_x, \delta g_y, \delta g_z, \sigma_x, \sigma_y$, and σ_z. Writing for the wave equations along the x axis, the extended scheme can be written here as

$$\frac{\partial f}{\partial t} = \sigma_x \cdot f + \frac{\partial g_x}{\partial x} + \sigma_x \cdot \delta g_x + s_x \tag{64}$$

$$\frac{\partial g_x}{\partial t} = \sigma_x \cdot g_x + \frac{\partial f}{\partial x} + \sigma_x \cdot \delta f_x (+nc) \tag{65}$$

$$\frac{\partial \delta f_x}{\partial t} = \sigma_x \cdot \delta f_x + \frac{\partial \delta g_x}{\partial x} + \sigma_x \cdot g_x \tag{66}$$

$$\frac{\partial \delta g_x}{\partial t} = \sigma_x \cdot \delta g_x + \frac{\partial \delta f_x}{\partial x} + \sigma_x \cdot f + s_x \tag{67}$$

$$s_x = (\sigma_y + \sigma_z) f + \frac{\partial g_y}{\partial y} + \frac{\partial g_z}{\partial z} + \sigma_y \cdot \delta g_y + \sigma_z \cdot \delta g_z + S.$$

The term *nc* is here to recall that a numerical correction (as described in the preceding section) has to be added once the system is discretized.

The complete scheme can be written then in vectorial notation as

$$\frac{\partial f}{\partial t} = (\sigma_x + \sigma_y + \sigma_z) f + \vec{\nabla}\cdot\vec{g} + \vec{\sigma}\cdot\delta\vec{g} + S \tag{68}$$

$$\frac{\partial \vec{g}}{\partial t} = \vec{\vec{\sigma}}\cdot\vec{g} + \vec{\nabla} f + \vec{\vec{\sigma}}\cdot\delta\vec{f}(+nc) \tag{69}$$

$$\frac{\partial \delta \vec{f}}{\partial t} = \vec{\vec{\sigma}}\cdot\delta\vec{f} + \vec{\vec{\nabla}}\cdot\delta\vec{g} + \vec{\vec{\sigma}}\cdot\vec{g} \tag{70}$$

$$\frac{\partial \delta \vec{g}}{\partial t} = \vec{\vec{\sigma}}\cdot\delta\vec{g} + \vec{\vec{\nabla}}\cdot\delta\vec{f} + \vec{\sigma} f + \vec{s} \tag{71}$$

$$\vec{s} = [(\sigma_x + \sigma_y + \sigma_z) f + \vec{\nabla} \cdot \vec{g} + \vec{\sigma} \cdot \delta\vec{g} + S]\hat{u} - (\vec{\sigma} f + \vec{\vec{\nabla}} \cdot \vec{g} + \vec{\vec{\sigma}} \cdot \delta\vec{g})$$
$$= \frac{\partial f}{\partial t}\hat{u} - (\vec{\sigma} f + \vec{\vec{\nabla}} \cdot \vec{g} + \vec{\vec{\sigma}} \cdot \delta\vec{g}), \tag{72}$$

where

$$\vec{\sigma} = \begin{pmatrix} \sigma_x \\ \sigma_y \\ \sigma_z \end{pmatrix} \quad \text{and} \quad \vec{\vec{\sigma}} = \begin{pmatrix} \sigma_x & 0 & 0 \\ 0 & \sigma_y & 0 \\ 0 & 0 & \sigma_z \end{pmatrix}.$$

Discretization. By reproducing the discretization described in the one-dimensional case by (45) and (46), we obtain the system

$$\Delta_t f = \sigma \langle f \rangle_t + \sum_{v=x}^{z} \Delta_v g_v + \sum_{v=x}^{z} \sigma_v \langle \delta g \rangle_v - S \tag{73}$$
$$\Delta_t g_u = \sigma_u \langle g_u \rangle_t + \Delta_u f + \sigma_u \langle \delta f_u \rangle_u - 0.5 \Delta_u F_u \tag{74}$$
$$\Delta_t \delta g_u = \sigma_u \langle \delta g_u \rangle_t + \Delta_u \delta f_u + \sigma_u \langle f \rangle_u - 2 \langle F_u \rangle_u \tag{75}$$
$$\Delta_t \delta f_u = \sigma_u \langle \delta f_u \rangle_t + \Delta_u \delta g_u + \sigma_u \langle g_u \rangle_u \tag{76}$$
$$s_u = (\sigma - \sigma_u) \langle f \rangle_t + \sum_{v=x}^{z} \Delta_v g_v + \sum_{v=x}^{z} \sigma_v \langle \delta g \rangle_v - \Delta_u g_u - \sigma_u \langle \delta g \rangle_u - S \tag{77}$$
$$\Delta_t F_u = 2 \cdot G_u / \delta u - s_u \tag{78}$$
$$\Delta_t G_u = -\frac{2}{\delta u} \langle G_u \rangle_t - 2 F_u / \delta u, \tag{79}$$

where we have introduced the additional variables F and G, and where $u = x$, y, or z, and $\sum_{v=x}^{z}$ means the sum for $v = x$, y, and z.

2.3. Application to Maxwell Equations

The Maxwell wave equations are

$$\begin{aligned} \frac{\partial \vec{B}}{\partial t} &= -\vec{\nabla} \times \vec{E} \\ \frac{\partial \vec{E}}{\partial t} &= \vec{\nabla} \times \vec{B} - \vec{J}, \end{aligned} \tag{80}$$

giving a "truncated" wave equation for the electric field

$$\frac{\partial^2 \vec{E}}{\partial t^2} = -\vec{\nabla} \times \vec{\nabla} \times \vec{E} - \frac{\partial \vec{J}}{\partial t}. \tag{81}$$

Because the algorithm we have developed applies to full wave equations, it is desirable to rebuild the Laplacian in the electric field wave equation, leading us to use

$$\frac{\partial^2 \vec{E}}{\partial t^2} = \vec{\nabla}(\vec{\nabla} \cdot \vec{E}) - \vec{\nabla} \times \vec{\nabla} \times \vec{E} - \frac{\partial \vec{J}}{\partial t} - \vec{\nabla}\rho = \Delta \vec{E} - \frac{\partial \vec{J}}{\partial t} - \vec{\nabla}\rho. \tag{82}$$

We can rewrite it as a system of first-order derivative equations as

$$\frac{\partial E_x}{\partial t} = \vec{\nabla} \cdot \vec{u} - J_x; \quad \frac{\partial \vec{u}}{\partial t} = \vec{\nabla} E_x - \begin{pmatrix} \rho \\ 0 \\ 0 \end{pmatrix} \tag{83}$$

(84)

$$\frac{\partial E_y}{\partial t} = \vec{\nabla} \cdot \vec{v} - J_y; \quad \frac{\partial \vec{v}}{\partial t} = \vec{\nabla} E_y - \begin{pmatrix} 0 \\ \rho \\ 0 \end{pmatrix} \tag{85}$$

(86)

$$\frac{\partial E_z}{\partial t} = \vec{\nabla} \cdot \vec{w} - J_z; \quad \frac{\partial \vec{w}}{\partial t} = \vec{\nabla} E_z - \begin{pmatrix} 0 \\ 0 \\ \rho \end{pmatrix}. \tag{87}$$

The extended scheme is applied independently on each 3D scalar wave equation on E_x, E_y, and E_z. The magnetic field, if needed (to push the particles in a particle-in-cell code for example), is extracted as

$$\begin{aligned} B_x &= v_z - w_y \\ B_y &= w_x - u_z \\ B_z &= u_y - v_x. \end{aligned} \tag{88}$$

2.4. Numerical Example

In Fig. 3, we display snapshots of the relaxation of a 2D (E_z, B_x, B_y) extended system in response to a source $J_z = H(t, 0) \cdot \delta(x_0, y_0)$, where $H(t, 0)$ are the Heaviside and the delta functions defined as

$$H(t, t_0) = \begin{cases} 1 & \text{when } t > t_0 \\ 0 & \text{otherwise} \end{cases} \tag{89}$$

$$\delta(x_0, y_0) = \begin{cases} 1 & \text{if } (x, y) = (x_0, y_0) \\ 0 & \text{otherwise} \end{cases} \tag{90}$$

and where (x_0, y_0) is located at the center of the grid. The moduli of E, B, δE, and δB are displayed for two runs with $\sigma = 0$ (left column) and $\sigma = -0.1/\delta x$ (right column), respectively. We can observe the smoothing that results from the damping of high frequencies when $\sigma < 0$. We can also verify that we effectively have $|E| = |\delta B|$ and $|B| = |\delta E|$. The possibility of adjusting the damping of high frequency by adjusting σ, and with it the speed of high-frequency waves (see Fig. 2), is clearly an advantage. It can be used to damp waves that have an unphysical behavior (simulation velocity lower than real velocity). This is an obvious benefit for electromagnetic simulations with relativistic particles where such waves can trigger numerical Cerenkov instabilities [7].

3. PART II: MESH REFINEMENT ALGORITHM FOR THE WAVE EQUATION

The extended scheme developed in Part I allows the implementation of a mesh refinement algorithm more naturally than the Yee scheme. We present in this part the boundary condition in 1D for the interface of two grids in which the extended scheme is used. An obvious

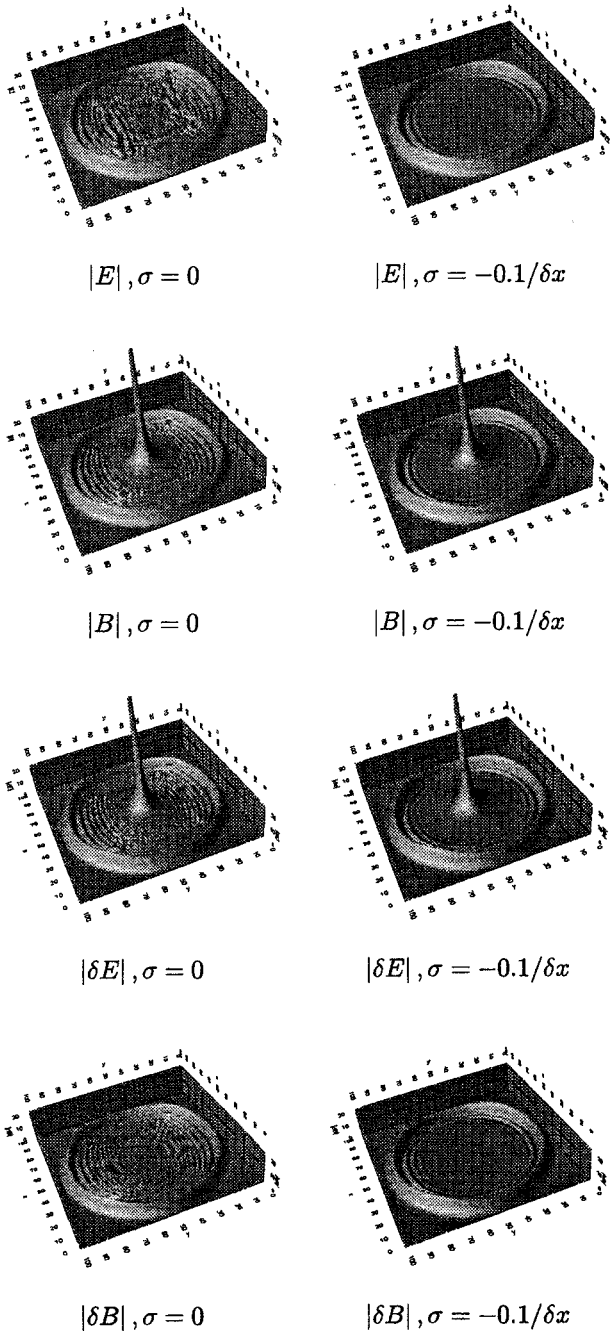

FIG. 3. Snapshots of the relaxation of a 2D (E_z, B_x, B_y) extended system in response to a source $J_z = H(t, 0) \cdot \delta(x_0, y_0)$ with (x_0, y_0) located at the center of the grid. The results of two runs are displayed for $\sigma = 0$ (left column) and $\sigma = -0.1/\delta x$ (right column).

problem in spatially varying the resolution is the treatment of short wavelengths, which can be resolved in a fine-gridded area but not in a coarser-gridded area. Using the fact that with the extended scheme, we can treat separately incoming and outcoming waves in different areas of the grid, we build an interface that filters such waves at the interface. This filtering

is fundamental in preventing instabilities often reported with mesh refinement algorithms. We present an algorithm first for spatial mesh refinement and then for space and time mesh refinement.

3.1. Spatial Refinement Only

We consider the interface of two grids having different resolutions and consider two solutions, for the waves going respectively forward $E^{(+)}$ and backward $E^{(-)}$ (cf. Fig. 4). The connection with the quantities of the extended scheme used inside the grids is done using (23).

We write the solutions as

$$E_j^{i+1} = E_j^{(+)i+1} + E_j^{(-)i+1} \tag{91}$$

$$E_j^{(+)i+1} = \alpha^{(+)} E_j^{(+)i} + \beta_u^{(+)} B_{j+1/2}^{(+)i+1/2} - \beta_l^{(+)} B_{j-1/2}^{(+)i+1/2} \tag{92}$$

$$= \left(1 + \beta_u^{(+)} - \beta_l^{(+)}\right) E_j^{(+)i} + \beta_u^{(+)} B_{j+1/2}^{(+)i+1/2} - \beta_l^{(+)} B_{j-1/2}^{(+)i+1/2} \tag{93}$$

$$E_j^{(-)i+1} = \alpha^{(-)} E_j^{(-)i} + \beta_u^{(-)} B_{j+1/2}^{(-)i+1/2} - \beta_l^{(-)} B_{j-1/2}^{(-)i+1/2} \tag{94}$$

$$= \left(1 - \beta_u^{(-)} + \beta_l^{(-)}\right) E_j^{(-)i} + \beta_u^{(-)} B_{j+1/2}^{(-)i+1/2} - \beta_l^{(-)} B_{j-1/2}^{(-)i+1/2}, \tag{95}$$

where $\alpha^{(\pm)}$, $\beta_u^{(\pm)}$, and $\beta_l^{(\pm)}$ are constant factors to be specified.

We consider the solution for the wave propagating forward only, the solution for the wave propagating backward being obtained by symmetry. We recall that, from the relation (18) linking the coefficients, we have

$$\alpha^{(+)} = 1 - \beta_l^{(+)} + \beta_u^{(+)}. \tag{96}$$

When the grids have the same resolution, we impose

$$\beta_u^{(+)} = \beta_l^{(+)} = \frac{\delta t}{\delta x}, \tag{97}$$

giving $\alpha^{(+)} = 1$.

When the second grid has a mesh size going to infinity ($\delta t/\delta x_2 \to 0$), we impose the algorithm to converge to the Sommerfeld outgoing-wave boundary condition at the interface of the first grid, giving

$$\alpha^{(+)} = 1 - \frac{2\alpha_1}{1 + \alpha_1} \tag{98}$$

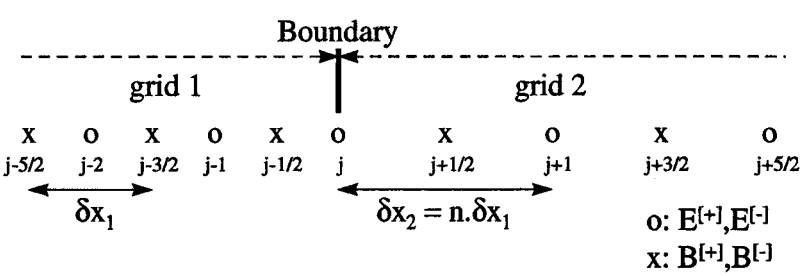

FIG. 4. Two uniform grids connected at location j. The mesh size of the second grid is n times the mesh size of the first grid. the electromagnetic field is separated in two parts: waves going forward ($E^{[+]}$, $B^{[+]}$) and backward ($E^{[-]}$, $B^{[-1]}$).

$$\beta_l^{(+)} = \frac{2\alpha_1}{1+\alpha_1} = \alpha_1\left(1+\frac{1-\alpha_1}{1+\alpha_1}\right) \tag{99}$$

$$\beta_u^{(+)} = 0 \tag{100}$$

$$\text{with} \quad \alpha_1 = \delta t/\delta x_1 \quad \text{and} \quad \alpha_2 = \delta t/\delta x_2. \tag{101}$$

Similarly, when the second grid has a mesh size going to 0, or, equivalently, when the first grid has a mesh size going to infinity ($\delta t/\delta x_1 \to 0$), we impose the algorithm to converge to an ingoing-wave boundary condition; that is

$$\alpha^{(+)} = 1 + \frac{2\alpha_2}{1-\alpha_2} \tag{102}$$

$$\beta_l^{(+)} = 0 \tag{103}$$

$$\beta_u^{(+)} = \frac{2\alpha_2}{1-\alpha_2} = \alpha_2\left(1+\frac{1+\alpha_2}{1-\alpha_2}\right). \tag{104}$$

The following set of solutions verifies these requirements:

$$\begin{aligned} \beta_l^{(+)} &= \alpha_1\left[1+\left(\frac{1-\alpha_1}{1+\alpha_1}\right)\left(\frac{\alpha_1-\alpha_2}{\alpha_1+\alpha_2}\right)\right] \\ \beta_u^{(+)} &= \alpha_2\left[1+\left(\frac{1+\alpha_2}{1-\alpha_2}\right)\left(\frac{\alpha_2-\alpha_1}{\alpha_1+\alpha_2}\right)\right]. \end{aligned} \tag{105}$$

These coefficients are used in (93). The coefficients $\beta_l^{(-)}$ and $\beta_u^{(-)}$ for use in (95) are obtained by symmetry.

Although other solutions verifying these requirements can be constructed, after a parametric study, this set has been found to be the most successful by the author and will be the only one considered in the paper.

3.2. Space–Time Mesh Refinement

It is also possible to refine in time as well as in space. We split the $(E^{(+)}, E^{(-)})$ solution at the interface in $(E_{[1]}^{(+)}, E_{[1]}^{(-)})$ and $(E_{[2]}^{(+)}, E_{[1]}^{(-)})$ belonging to the first and second grid, respectively, and will consider a mesh refinement of $1:2$ ($\delta x_2 = 2\delta x_1$). Nothing changes inside each grid except that with the coarse grid we now use the time step $\delta t_2 = 2\delta t_1$, where δt_1 is the time step used with the fine grid. The values at the interface of the coarse grid $(E_2^{(+)}, E_2^{(-)})$ are computed by using the required values beyond the interface in the fine grid, jumping the unnecessary values (see Fig. 5). The values of $E_1^{(-)}$ (direction coarse-to-fine) are computed with the same algorithm as in the preceding section, using interpolated values from the coarse grid. The values of $E_1^{(+)}$ (direction coarse-to-fine) are the values of $E_2^{(-)}$ when available at the considered time step or are interpolated from them otherwise.

The finite-difference formulation of the overall scheme is given for one time step by (given for both $E^{(+)}$ and $E^{(-)}$)

1. $B^{i-1/2} \to B^{i+1/2}$; $\delta B^{i-1/2} \to \delta B^{i+1/2}$ inside fine grid using (45)
2. $B_{j+1/2}^{i+1/2} = 0.25B^{i-1} + 0.75B^{i+1}$; $\delta B_{j+1/2}^{i+1/2} = 0.25\delta B^{i-1} + 0.75\delta B^{i+1}$

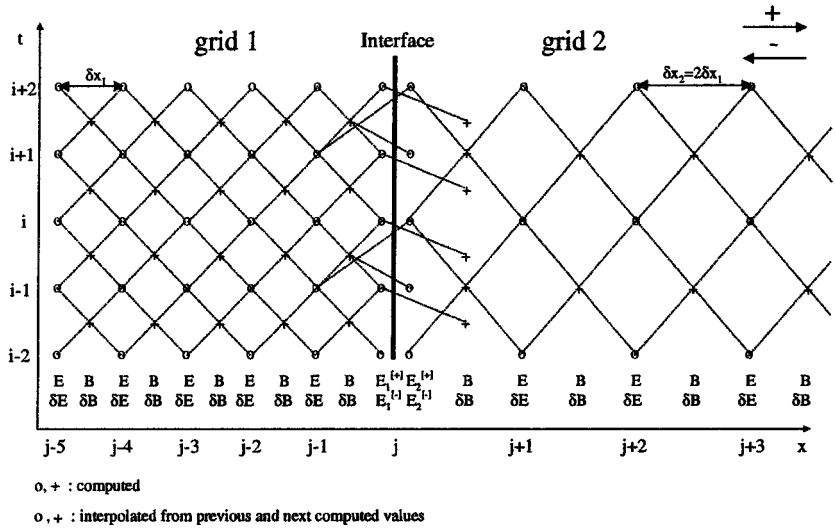

FIG. 5. Space–time diagram of the space–time mesh refinement scheme given as a visual aid to the reader (see text for explanations).

3. $E^i \to E^{i+1}$; $\delta E^i \to \delta E^{i+1}$ inside fine grid using (45)
4. $E^i \to E^{i+2}$; $\delta E^i \to \delta E^{i+2}$ inside coarse grid using (45)
5. $E_{[2]j}^{(+)i+2} = E_{[2]j}^{(+)i} + \frac{\delta t_2}{\delta x_2}(B_{j+1/2}^{(+)i+1} + E_{j-1}^{(+)i+1})$
6. $E_{[2]j}^{(-)i+2} = E_{[2]j}^{(-)i} + \frac{\delta t_2}{\delta x_2}(B_{j+1/2}^{(-)i+1} - E_{j-1}^{(-)i+1})$
7. $E_{[1]j}^{(+)i+1} = (1 + \beta_u^{(+)} - \beta_l^{(+)})E_{[1]j}^{(+)i} + \beta_u^{(+)} B_{j+1/2}^{(+)i+1/2} - \beta_l^{(+)} B_{j-1/2}^{(+)i+1/2}$ with

$$\begin{cases} \beta_l^{(+)} = \alpha_1 \left[1 + \left(\frac{1-\alpha_1}{1+\alpha_1}\right)\left(\frac{\alpha_1-\alpha_2}{\alpha_1+\alpha_2}\right)\right] \\ \beta_u^{(+)} = \alpha_2 \left[1 + \left(\frac{1+\alpha_2}{1-\alpha_2}\right)\left(\frac{\alpha_2-\alpha_1}{\alpha_1+\alpha_2}\right)\right], \end{cases} \tag{106}$$

where $\alpha_1 = \delta t_1/\delta x_1$ and $\alpha_2 = \delta t_1/\delta x_2$,

8. $E_{[1]j}^{(-)i+1} = 0.5(E_{[2]j}^{(-)i} + E_{[2]j}^{(-)i+2})$
9. $B^{i+1} \to B^{i+3}$; $\delta B^{i+1} \to \delta B^{i+3}$ inside coarse grid using (45)
10. $B^{i+1/2} \to B^{i+3/2}$; $\delta B^{i+1/2} \to \delta B^{i+3/2}$ inside fine grid using (45)
11. $B_{j+1/2}^{i+3/2} = 0.75B^{i+1} + 0.25B^{i+3}$; $\delta B_{j+1/2}^{i+3/2} = 0.75\delta B^{i+1} + 0.25\delta B^{i+3}$
12. $E^{i+1} \to E^{i+2}$; $\delta E^{i+1} \to \delta E^{i+2}$ inside fine grid using (45)
13. $E_{[1]j}^{(+)i+2} = (1 + \beta_u^{(+)} - \beta_l^{(+)})E_{[1]j}^{(+)i+1} + \beta_u^{(+)} B_{j+1/2}^{(+)i+3/2} - \beta_l^{(+)} B_{j-1/2}^{(+)i+3/2}$
14. $E_{[1]j}^{(-)i+2} = E_{[2]j}^{(-)i+2}$

Figure 5 is of great help in following the steps. Steps 1, 3, 4, 9, 10, and 12 concern the calculations of the extended scheme inside the fine and coarse grids. Steps 2, 8, 11, and 14 are interpolations in time of values needed on the fine grid from values known on the coarse grid. Steps 5, 6, 7, and 13 compute boundary values.

3.3. Coefficient of Reflection Measurements

We present results obtained with the interface (93), with (105), for the connection of two grids. The evolution of the coefficient of reflections and of transmission with respect to the pulsation ω due to the interface was computed using the following procedure.

At the left end of the first grid, the field E was imposed to be $E(\omega, t) = H(t)\sin(\omega t)$, where $H(t)$ is a Harris function defined as

$$H(t) = \begin{cases} \frac{10 - 15\cos(2\pi Lt) + 6\cos(4\pi Lt) - \cos(6\pi Lt)}{32} & \text{when } 0 < t < L/c \\ 0 & \text{otherwise,} \end{cases} \tag{107}$$

with $L = \frac{1}{n_{g1}}$ and c the speed of waves. This choice of $E(\omega, t)$ is to generate a quasi-monochromatic signal. Figures 6 and 7 display H(t), E(ω, t) and its Fourier transform $E^*(\omega, t)$.

Let the number of meshes for the first grid be n_{g1} and L_1 be its length. In the case where $\delta x_1 < \delta x_2$, the length of the second grid was chosen to be $L_2 = L_1$ while it was $L_2 = 1.5L_1$ otherwise. The number of meshes of the second grid was then $n_{g2} = L_2/\delta x_2$.

The results obtained on the system of two grids ((E_1, B_1) and (E_2, B_2)) were compared to those obtained under the same initial conditions on a grid of reference $(E_{\text{ref}}, B_{\text{ref}})$ having the same resolution as the first grid. The coefficient of reflection was computed as

$$R = \sqrt{\frac{\sum_{j=1}^{n_{g1}}[(E_1(j) - E_{\text{ref}}(j))^2 + (B_1(j) - B_{\text{ref}}(j))^2]\delta x_1}{\sum_{j=1}^{n_{g1}}[(E_{\text{ref}}(j))^2 + (B_{\text{ref}}(j))^2]\delta x_1}}, \tag{108}$$

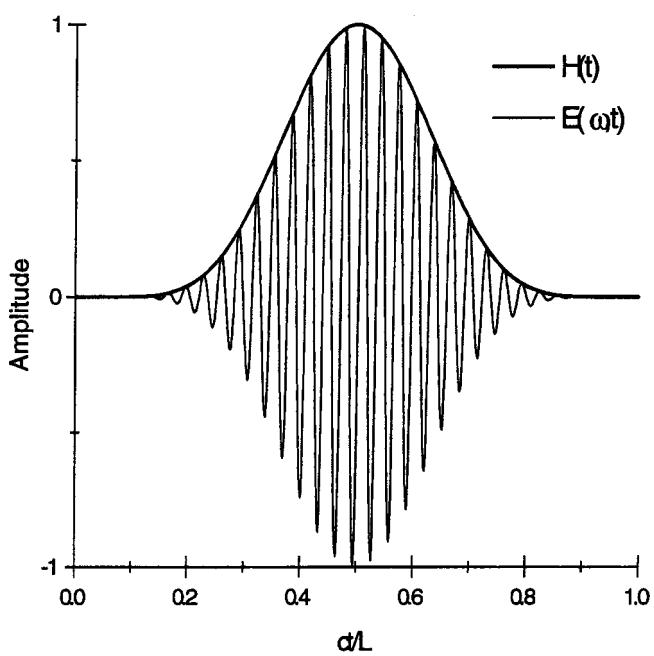

FIG. 6. The Harris function $H(t)$ and $E(\omega, t)$ plotted versus time.

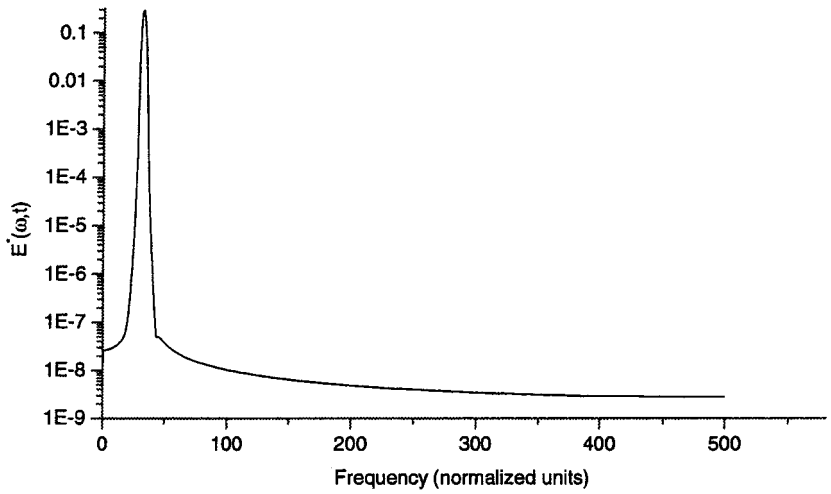

FIG. 7. The Fourier transform of $E(\omega, t)$ shows that the signal is nearly monochromatic.

while the coefficient of transmission was computed as

$$T = \sqrt{\frac{\sum_{j=1}^{n_{g2}}[(E_2(j))^2 + (B_2(j))^2]\delta x_2}{\sum_{j=n_{g1}+1}^{2n_{g1}}[(E_{\text{ref}}(j))^2 + (B_{\text{ref}}(j))^2]\delta x_1}}. \tag{109}$$

In all the calculations, the time t is initialized to 0 at the beginning of the run, and the time step $\delta t = 0.5\delta x_{\text{fine grid}}$ is used. The run ended at $t_{\max} = 2L_1/c(\omega)$, where $c(E(\omega))$ is the velocity of the pulse $E(\omega)$ at the pulsation ω. It was empirically determined that $c(E(\omega)) \approx (2./\delta x)\arcsin[(\delta x/\delta t)\sin(\omega'\delta t/2)]/\omega'$ with $\omega' = 1.3\omega$.

In order to validate the measurement procedure, the coefficient of reflection was also computed analytically as follows. For a wave of the form $E_0 e^{i(\omega t - kx)}$ propagating at the interface, and considering a coefficient of reflection r, we have, using Eq. (92) (we dropped the $^{(+)}$)

$$\begin{aligned}(1-r)e^{i\omega\delta t/2} = {} & (1-r)\alpha e^{-i\omega\delta t/2} - (1-r)\beta_u e^{-ik_2(\omega)\delta x_2/2} \\ & + \beta_l e^{ik_1(\omega)\delta x_1/2} + r\beta_l e^{-ik_1(\omega)\delta x_1/2},\end{aligned} \tag{110}$$

giving

$$|r| = \left| \frac{e^{i\omega\delta t/2} - \alpha e^{-i\omega\delta t/2} + \beta_u e^{-ik_2(\omega)\delta x_2/2} - \beta_l e^{ik_1(\omega)\delta x_1/2}}{e^{i\omega\delta t/2} - \alpha e^{-i\omega\delta t/2} + \beta_u e^{-ik_2(\omega)\delta x_2/2} + \beta_l e^{-ik_1(\omega)\delta x_1/2}} \right|. \tag{111}$$

The unknown $k_1(\omega)$ and $k_2(\omega)$ are obtained by solving the relation of dispersion in the first and second grid, respectively, as for (51), and are given by

$$k_1(\omega) = \frac{-2i}{\delta x_1} \ln\left[0.5\left(\delta x_1 B + \sqrt{\delta x_1^2 B^2 + 4}\right)\right] \tag{112}$$

$$k_2(\omega) = \frac{-2i}{\delta x_2} \ln\left[0.5\left(\delta x_2 B + \sqrt{\delta x_2^2 B^2 + 4}\right)\right] \tag{113}$$

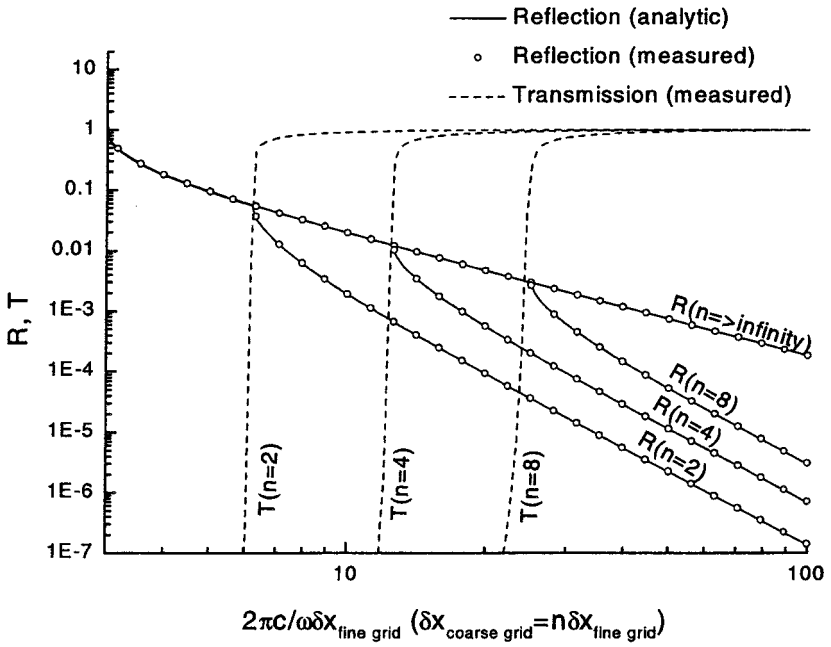

FIG. 8. Coefficients of reflection and transmission as a function of frequency at the interface between two grids having different resolutions for a wave traveling in the direction fine-to-coarse. Three refinements, 1 : 2, 1 : 4, and 1 : 8, are considered, as well as the limit case $1:\infty$ for which the algorithm tends to the one-way absorbing boundary algorithm.

with

$$B = \frac{\left(e^{i\omega\delta t/2} - e^{-i\omega\delta t/2}\right)}{\delta t}. \tag{114}$$

The coefficients of transmission and of reflection are given in Fig. 8 for the interface when the second grid has a lower resolution ($\delta x_2 = n\delta x_1$, $n = 2, 4, 8, \infty$) than the first grid. In the case $n \to \infty$, the algorithm has for a limit the one-way outgoing-wave boundary condition. In each of the other cases, it is remarkable to notice that we obtain the same coefficient of reflection as with the outgoing-wave algorithm for wavelengths below the cutoff of the second grid. For wavelengths above this cutoff, the coefficient of reflection is notably reduced by our algorithm compared to the outgoing-wave algorithm.

The case where the second grid has a higher resolution than the first one ($\delta x_2 = \delta x_1/n$, $n = 2, 4$) is displayed in Fig. 9 and Fig. 10. Our algorithm gives a smaller coefficient of reflection than the outgoing-wave boundary condition, and it amplifies the transmitted signal up to about 20% at the shortest wavelength, while the outgoing-wave boundary condition damps the signal at a slower rate.

The coefficients of reflection and transmission have also been measured in the case of the space-time mesh-refinement; the results are given in Fig. 11 for both direction (fine-to-coarse and coarse-to-fine).

3.4. Comparison with Other Schemes

3.4.1. *Space Refinement Only*

The easiest way to build an interface between two grids having different resolutions is to use a contour path extension of the Yee scheme [5], giving as a solution at the interface

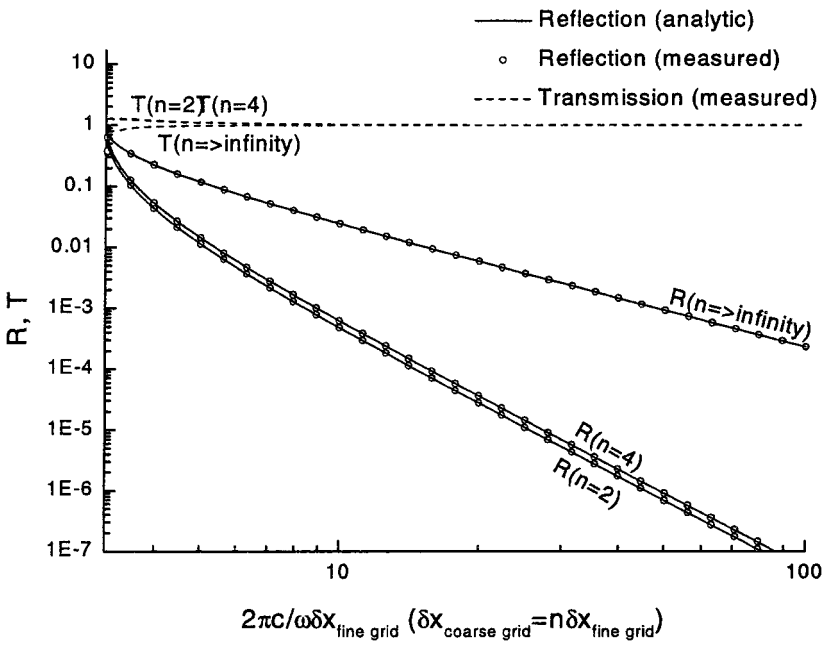

FIG. 9. Coefficients of reflection and transmission as a function of frequency at the interface between two grids having different resolutions, for a wave traveling in the direction coarse-to-fine. Two refinements, 1 : 2 and 1 : 4, are considered. The coefficients due to connecting the grids with a one-way absorbing boundary condition algorithm are also given as a reference.

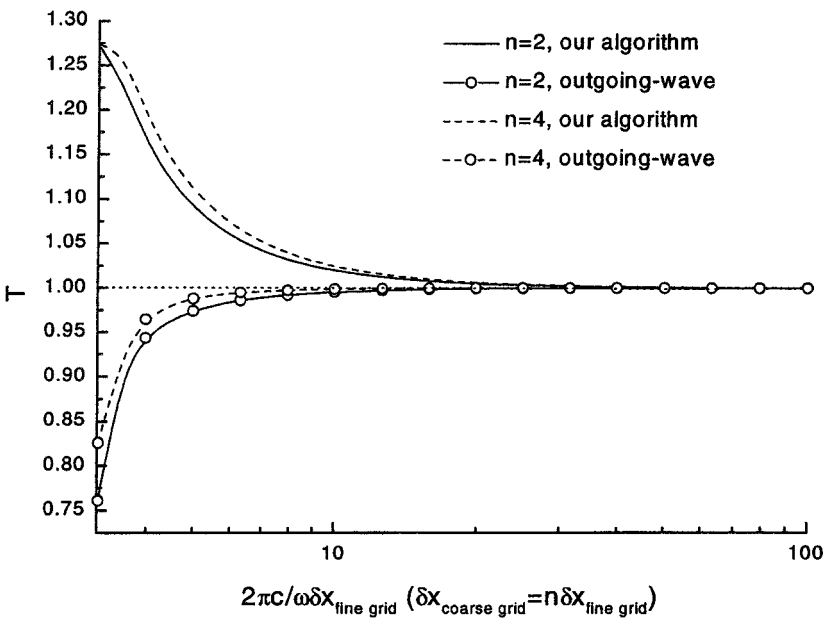

FIG. 10. Same as preceding figure but transmission coefficients only, with a different scale. At high frequencies, our scheme amplifies the signal up to about 20% while a connection with the outgoing-wave boundary condition damps the signal at about the same rate.

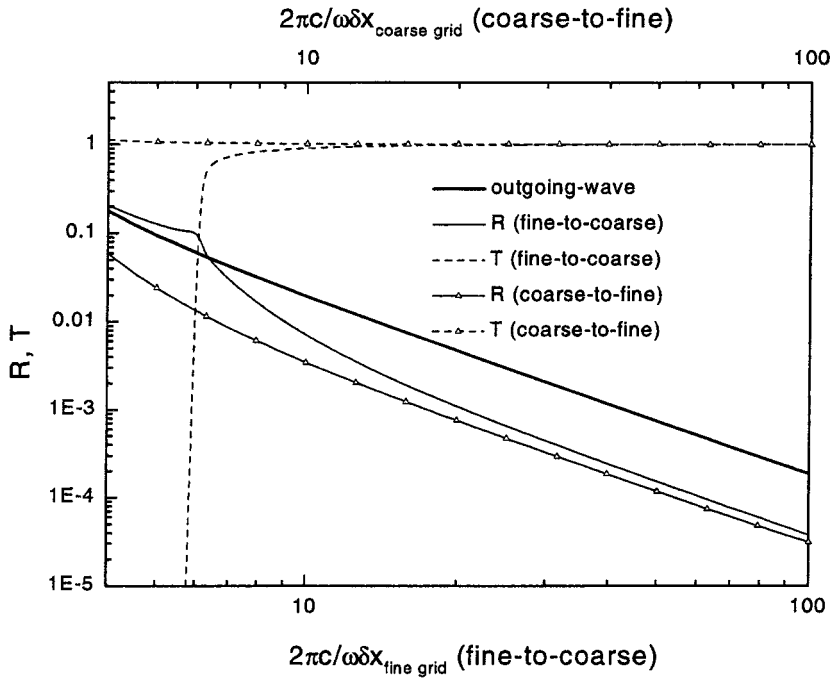

FIG. 11. Coefficients of reflection and transmission for a connection of two grids with space–time refinement 1 : 2. The lower axis corresponds to the measurement for waves traveling in the direction fine-to-coarse. The upper axis corresponds to the coarse-to-fine measurements.

$$\frac{E_j^{i+1} - E_j^i}{\delta t} = \frac{B_{j+1/2}^{i+1/2} - B_{j-1/2}^{i+1/2}}{0.5(\delta x_{\text{fine}} + \delta x_{\text{coarse}})}. \tag{115}$$

Another way, for a mesh refinement of $1:n$ with n odd, if one desires to have a centered finite difference at the interface, is to compute the solution with the δx of the coarse grid, jumping to the required value in the fine grid, giving

$$\frac{E_j^{i+1} - E_j^i}{\delta t} = \frac{B_{j+1/2}^{i+1/2} - B_{j-n/2}^{i+1/2}}{\delta x_{\text{coarse}}}. \tag{116}$$

For a mesh refinement 1 : 3, the coefficients of reflection were measured for these two schemes (contour path and "jump") in the direction fine-to-coarse and are compared with our new scheme in Fig. 12. We observe that these two schemes give very similar results and give an amount of reflection significantly larger than our scheme. Especially, they both produce a coefficient larger than 1 for at least part (if not all) of the frequencies above the cutoff of the coarse grid. This is a serious problem when considering a sandwich configuration where a fine grid is embedded between two coarse grids (very likely in practice) because these frequencies drive then an instability by multiple reflection with amplification at the interfaces.

3.4.2. *Space–Time Refinement*

The first scheme we consider, for refinement $1:n$ with n odd, uses the solution of the coarse grid computed by jumping to the required component in the fine grid, as we

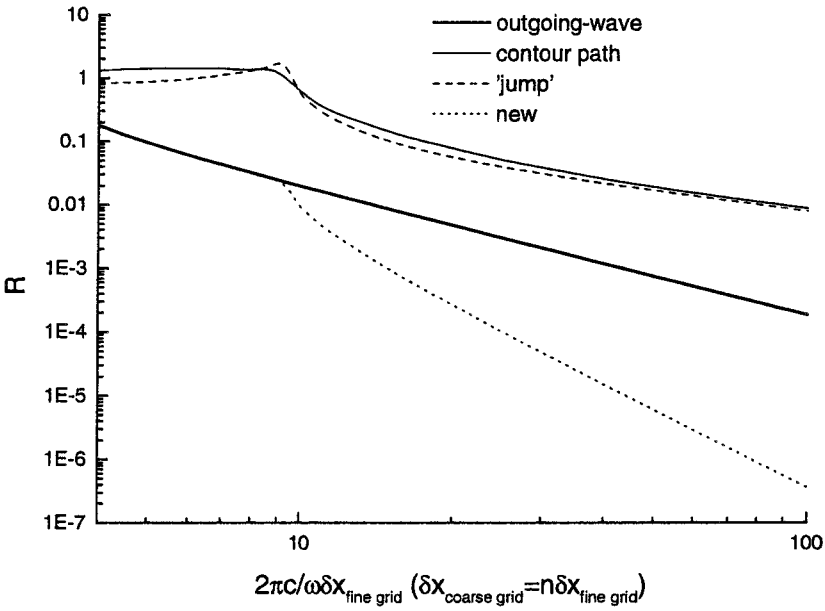

FIG. 12. Coefficients of reflection for space mesh refinement schemes in the direction fine-to-coarse. The contour path and jump schemes both give at high frequencies reflections of waves with amplification that would drive an instability in the case of a sandwich configuration.

did to compute the solution "coarse-to-fine" on the coarse grid in our space–time refinement scheme. The solution on the fine grid is then simply interpolated in time (as we did to compute the solution "coarse-to-fine" on the fine grid in our space–time refinement scheme).

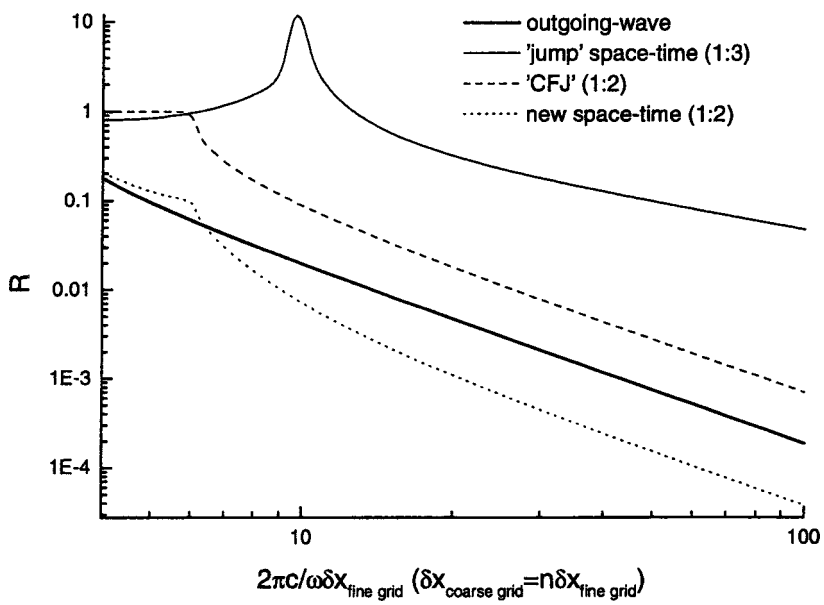

FIG. 13. Coefficients of reflection of space–time mesh refinement schemes. The new scheme notably reduces the amount of reflection compared to other schemes.

Another scheme proposed in [4] derives a local solution at the interface by imposing conservation of energy at the discrete level to the whole system (fine grid + interface + coarse grid). The result is an interface for which the sum of the coefficient of reflection and transmission is always 1 (with none of them negative), making the system stable.

The coefficients of reflection were measured for these two schemes in the direction fine-to-coarse and are compared with our new scheme for space–time refinement in Fig. 13. The first scheme gives a very strong reflection near the cutoff frequency of the coarse grid with an amplification of the wave up to approximately 10. This scheme will thus be very unstable for a sandwich configuration. As expected with the energy-conserving scheme, the waves with a frequency above the cutoff of the coarse grid are completely reflected. This means that even if the high-frequency waves will not grow in the fine-gridded region, they will be trapped and if there is a source of waves with components at these frequencies, they will build up in the fine region.

4. CONCLUSION

In this paper, we have proposed a general form to approximate the wave equation in centered finite difference depending, for the simplest possible subset, on three constant parameters to be determined. A relation linking the parameters has been derived, and it is shown that, unless specific conditions apply, this relation differs according to the direction of wave propagation. To develop a scheme compatible with any possible set of parameters, we have developed an "extended" scheme, operating on a linear combination of the components propagating forward and backward, respectively, along an axis of the system. A boundary condition for accommodating the mesh refinement technique with the extended scheme has been developed in 1D and has been compared to other existing schemes. The numerical results show that the reflections produced at the interface are very small. The results obtained in 1D are very promising, and the extension of this boundary condition to 2D and 3D will be treated in a paper to follow. An article describing an interface between the extended scheme and the Yee scheme is also in preparation.

APPENDIX

Correction Term for the Extended Scheme

The extended scheme is

$$\begin{aligned}
\frac{\partial B}{\partial t} &= \sigma_B B + \frac{\partial E}{\partial x} + \sigma_B \delta E \\
\frac{\partial E}{\partial t} &= \sigma_E E + \frac{\partial B}{\partial x} + \sigma_E \delta B - J \\
\frac{\partial \delta E}{\partial t} &= \sigma_E \delta E + \frac{\partial \delta B}{\partial x} + \sigma_E B \\
\frac{\partial \delta B}{\partial t} &= \sigma_B \delta B + \frac{\partial \delta E}{\partial x} + \sigma_B E + J,
\end{aligned} \tag{A.1}$$

which can be discretized as

$$\begin{aligned}
\Delta_t B &= \sigma_B \langle B \rangle_t + \Delta_x E + \sigma_B \langle \delta E \rangle_x \\
\Delta_t E &= \sigma_E \langle E \rangle_t + \Delta_x B + \sigma_E \langle \delta B \rangle_x - J \\
\Delta_t \delta E &= \sigma_E \langle \delta E \rangle_t + \Delta_x \delta B + \sigma_E \langle B \rangle_x \\
\Delta_t \delta B &= \sigma_B \langle \delta B \rangle_t + \Delta_x \delta E + \sigma_B \langle E \rangle_x + \langle \langle J \rangle_x \rangle_t .
\end{aligned} \tag{A.2}$$

At the infinitesimal limit ($\delta t \to 0, \delta x \to 0$), this system must converge to (A.1) and thus must verify at this limit (recalling that, by definition, $\delta E = -B$ and $\delta B = -E$)

$$\begin{aligned}
\langle B \rangle_t &= -\langle \delta E \rangle_x \\
\langle E \rangle_t &= -\langle \delta B \rangle_x \\
\langle \delta E \rangle_t &= -\langle B \rangle_x \\
\langle \delta B \rangle_t &= -\langle E \rangle_x .
\end{aligned} \tag{A.3}$$

The infinitesimal limit means that any signal Fourier component must have its wavelength and period covering an infinite number of meshes and an infinite number of time steps, respectively. This limit is attainable by the discretized system only for a steady state. Considering thus the discretized system in a steady state with a source $J = 1$ located at $j = 0$, we have

j	$-3/2$	-1	$-1/2$	0	$1/2$	1	$3/2$
J		0		1		0	
$\langle B \rangle_t = B$	-1		-1		1		1
$\langle E \rangle_t = E$		-1		-1		-1	
$\langle \delta B \rangle_t = \delta B$	1		1		1		1
$\langle \delta E \rangle_t = \delta E$		1		0		1	
$\langle \delta E \rangle_x$	1		0.5		-0.5		-1
$\langle \delta B \rangle_x$		1		1		1	
$\langle B \rangle_x$	-1		-1		-1		-1
$\langle E \rangle_x$		-1		0		1	

The condition $\langle B \rangle_t = -\langle \delta E \rangle_x$ is obviously not fulfilled, and a correcting term has to be added to the system, which becomes

$$\begin{aligned}
\Delta_t B &= \sigma_B \langle B \rangle_t + \Delta_x E + \sigma_B \langle \delta E \rangle_x + 0.5 \sigma_B \Delta_x \langle J \rangle_t \\
\Delta_t E &= \sigma_E \langle E \rangle_t + \Delta_x B + \sigma_E \langle \delta B \rangle_x - J \\
\Delta_t \delta E &= \sigma_E \langle \delta E \rangle_t + \Delta_x \delta B + \sigma_E \langle B \rangle_x \\
\Delta_t \delta B &= \sigma_B \langle \delta B \rangle_t + \Delta_x \delta E + \sigma_B \langle E \rangle_x + \langle \langle J \rangle_x \rangle_t .
\end{aligned} \tag{A.4}$$

ACKNOWLEDGMENTS

The author thanks J. C. Adam, W. Fawley, T. Fouquet, A. Friedman, D. Grote, A. Héron, P. Joly, and E. Sonnendrucker for many useful discussions and comments.

REFERENCES

1. J. P. Bérenger, A perfectly matched layer for the absorption of electromagnetic waves, *J. Comput. Phys.* **114**, 185 (1994).
2. K. S. Yee, Numerical solution of initial boundary value problems involving Maxwell's equations in isotropic media, *IEEE Trans. Antennas Propag.* **14**, 302 (1966).
3. B. Engquist and A. Majda, Absorbing boundary conditions for the numerical simulation of waves, *Math. Comput.* **31**, 629 (1977).
4. F. Collino, T. Fouquet, and P. Joly, Une méthode de raffinement de maillage espace-temps pour le système de Maxwell en dimension un, *C.R. Acad. Sci. Paris* **328**, 263 (1999).
5. A. Taflove, *Advances in Computational Electrodynamics: The Finite-Difference Time-Domain Method* (Artech House, Norwood, MA, 1998).
6. B. Gustafson, H.-O. Kreiss, and J. Oliger, *Time Dependent Problems and Difference Methods* (Wiley, New York, 1995), p. 52.
7. C. K. Birdsall and A. B. Langdon, *Plasma Physics via Computer Simulation* (Adam Hilger, New York, 1991), p. 355.